NASA TECHNICAL TRANSLATION NASA TT F-15,729

INVESTIGATIONS ON ROLLING DAMPING OF SLENDER WINGS

F. Schlottmann

Translation of "Untersuchungen der rolldämpfung von schlanken flügeln," Institute for Thermodynamics and Fluid Dynamics, Ruhr University, West Germany, Report 71-078, 1971, 20 pp.

NATIONAL AERONAUTICS AND SPACE ADMINISTRATION
WASHINGTON, D.C. 20546 JUNE 1974

STANDARD TITLE PAGE

1. Report No. NASA TT F-15,729	2. Government Accession No.	3. Recipient's Catalog No.
4. Title and Subtitle INVESTIGATIONS ON ROLLING DAMPING OF SLENDER WINGS		5. Report Date June 1974 6. Performing Organization Code
7. Author(s) F. Schlottmann, Institute for Thermodynamics and Fluid Dynamics, Ruhr University, Bochum		8. Performing Organization Report No. 10. Work Unit No. 11. Contract or Grant No. NASw-2481
9. Performing Organization Name and Address Leo Kanner Associates, P.O. Box 5187, Redwood City, California 94063		13. Type of Report and Period Covered Translation
12. Sponsoring Agency Name and Address NATIONAL AERONAUTICS AND SPACE ADMINISTRATION, WASHINGTON, D.C. 20546		14. Sponsoring Agency Code

15. Supplementary Notes

Translation of "Untersuchungen der rolldämpfung von schlanken flügeln," Institute for Thermodynamics and Fluid Dynamics, Ruhr University, West Germany, Report 71-078, 1971, 20 pp.

16. Abstract

The aerodynamic forces acting upon slender wing configurations in roll were measured in a low-speed wind tunnel in order to determine the influence of variation of angle of attack and roll angular velocity. It was shown, for the delta- and square-wing models investigated, that a nonlinear relationship exists between rolling moment and roll angular velocity, and relationship between roll damping and angle of attack. The reason for this is the presence of the leading-edge separation together with the formation of rolled-up vortices over the wing plane. The different vortex configurations and the resulting effects on roll damping are discussed, and compared with the theory.

17. Key Words (Selected by Author(s))	18. Distribution Statement
	Unclassified - Unlimited

19. Security Classif. (of this report)	20. Security Classif. (of this page)	21. No. of Pages	22. Price
Unclassified	Unclassified	~~20~~ 22	

INVESTIGATIONS ON ROLLING DAMPING OF SLENDER WINGS

F. Schlottmann
Institute for Thermodynamics and Fluid Dynamics, Ruhr University

1. Introduction /1*

The development of supersonic aircraft has led to the employment of slender wing configurations with sharp leading edges. For such wings, it is known that the aerodynamic forces vary nonlinearly with the angle of attack. The pitched slender wing in symmetrical flow has already been thoroughly studied, both theoretically and experimentally. See e.g. [1, 2].

The cause for the nonlinear behavior is the separation of flow from the leading edges or lateral edges even at small angles of attack. Two vortex layers develop, which roll up above the suction side of the wing into conical, concentrated vortices (Fig. 1). The overspeeds induced by these vortices at the wing surface are the cause for the additional peaks in the pressure distribution, which can result in a nonlinear lift characteristic. While the associated flow configurations have very frequently been the subject of publications, no systematic studies have yet been reported on moving -- i.e. rotating or oscillating -- wings with respect to the nonlinear behavior of the aerodynamic coefficients. This is because of the difficulties involved with measuring aerodynamic forces on moving models.

Since, in contrast to classical wings of large aspect ratio, the moment of inertia of a slender wing about the longitudinal axis is relatively small, the aerodynamic properties crucial for the roll motion are of great importance. This is particularly true for rolling damping, the aerodynamic moment opposing

*Numbers in the margin indicate pagination in the foreign text.

the rolling motion, since it is particularly small for slender wings. It is therefore necessary to come up with particularly precise figures on rolling damping and also to study it in relation to any possible nonlinear behavior.

Experiments carried out in England [3] have confirmed the /2
hypothesis that separation phenomena also occur at the sharp leading edges of rolling slender wings. Due to the antisymmetric angle-of-attack distribution in the span direction caused by the rolling motion, the configuration of the separated vortex layers is antisymmetric and no longer conical as in the case of the constant angle of attack (Fig. 2).

Nevertheless, there are still no quantitative figures for simple wing configurations with the variation of several parameters such as angle of attack α and roll angular velocity ω_x. In order to remedy this lack of systematic studies, the properties of slender wings in rolling motion were studied experimentally and theoretically at the Institute for Thermodynamics and Fluid Dynamics of Ruhr University. A particular objective was to study the extent to which rolling damping exhibited a nonlinear dependence on the roll angular velocity Ω_x.

2. Description of the Experiment Apparatus

A system was set up to permit steady roll motion of the wing models in the throat of a low-speed wind tunnel. In order to obtain steady flow around the rolling model even for angles of attack different from zero, the axis of rotation must remain fixed, coinciding with the direction of the airstream, as the angle of attack is varied. For this reason, the angle of attack cannot be shifted just by tipping the entire drive aggregate. Instead, this must be done on the rotating shaft.

This requirement results in an apparatus depicted schematically in Fig. 3. It is a rolling balance of the type already constructed by the firm Entwicklungsring Süd [4].

The wing model with the built-in strain gauge balance for /3
the rolling moment is rotated by the drive shaft via a parallelogram linkage. The shaft is mounted on a stable frame by means of two bearing blocks and is driven via a V-belt by a motor located beneath the wind jet via a servomechanism. With the aid of this drive aggregate, the speed of rotation of the model can be adjusted continuously between 10 and 300 rpm. The rotational speed is measured by means of a pulse technique. Light and dark marks situated on the V-belt pulley are scanned by a photoelectric tachometer, which delivers pulses with a frequency proportional to the rate of revolution.

The parallelogram linkage, which turns with the shaft, makes it possible to adjust the angle of attack in such a fashion that the reference point of the model for all angles of attack is on the axis of rotation.

The bending of the parallelogram linkage to adjust the angle of attack is produced by shifting an adjusting nut on a threaded sleeve, which is rotated via a servomotor. In this way, both the angle of attack and the roll angular velocity can be changed when the wind tunnel is operating and rotation is already occurring, and this substantially simplifies the execution of the experiments.

As the parallelogram linkage bends, a rod on which a counterweight is located and movable swings out in the opposite direction. By attaching suitable counterweights, the imbalances can be kept small with the aid of this arrangement over the entire angle-of-attack adjustment range of 0° to about 30°. At the lower

end of the shaft there is a slip-ring contact, which transmits the electrical signals measured on the rotating shaft to the stationary environment.

Since rolling damping assumes particularly small values /4 for slender wings, measuring it requires very sensitive measuring balances, whose readings must not be affected by other aeodynamic-force components or the large centrifugal forces produced by the rotation. For this reason, it is appropriate to deviate from the standard construction principle for strain-gauge balances, that of manufacturing the entire balance from a single piece. In that case, it would have to be anticipated that the interference in the rolling moment measurement due to the large transverse forces would attain the same order of magnitude as the rolling moment measurement itself.

To measure the rolling moment, a strain-gauge balance was employed which uses ball bearings as the transfer elements. The balance depicted schematically in Fig. 4 consists of a shaft and a sleeve mounted on it by means of two ball bearings, the wing model being pushed onto the sleeve. All forces and moments with the exception of the rolling moment are transferred by the ball bearings directly from the model to the shaft. The rolling moment, which acts about the axis of rotation of the ball bearings, is picked up by a measuring spring and generates a proportional electrical voltage with the aid of the strain gauge. No measurable transverse-component influences were detected in sample measurements with this arrangement. Since transmission of the measurement voltages from the rotating shaft to the stationary environment with the aid of a slip-ring contact is required, four strain gauges had to be arranged on the measuring spring in the form of a full-wave bridge rectifier. In this way, interferences due to the slip-ring-brush contact can be avoided.

To register the electrical voltages proportional to the measurements and the sequence of pulses stemming from the angular-velocity measurement, a data-recording unit was employed which punches the measurements onto cards, this permitting subsequent analysis on an electronic computer.

3. Experimental Program

/5

Rolling moment was measured on several wings with the side ratio $\Lambda = 1$ with the tapers $\lambda = l_a/[\text{illeg.}] = 0$ (triangular wing), 0.125, 0.5, and 1 (square wing). Because of the space required for the measuring balance, the middle section of the wing had a circular-arc profile with a relative thickness of 8% (for $\lambda = 0$ and 0.125) or 10% (for $\lambda = 0.5$ and 1.0), the profiles being extended in straight lines to the lateral edge. To hold the measuring balance, the wings were equipped with a tubular fuselage near the back. These models were made of fiberglass-reinforced polyester resin.

In order to obtain an estimate on the effect of thickness, a triangular wing made of an aluminum sheet 2 mm thick with sharp edges and a fuselage with an elliptic cross section was also employed.

The measurements were taken in the throat of the 1.3-m-diameter wind tunnel in the Fluid Mechanics Institute of the University of Braunschweig. A special collecting cone equipped with appropriate recesses was prepared for the roll balance, permitting the partial installation of the frame for the apparatus of the experiment into the collecting cone. This arrangement is depicted in Fig. 5.

The Reynolds number, relative to the reference chord depth $l_u = A^{-1}\int_{-s}^{+s} l^2(y)dy$, was $Re = 1.04 \cdot 10^6$ for all wings employed.

The angle of attack varied betwen $\alpha = 0°$ and $\alpha = 30°$. The dimensionless angular velocity $\Omega_x = \omega_x s/v$ of the roll motion varied between $\Omega_x = 0$ and 0.1.

4. Results

/6

In taking the measurements, the entire range of roll angular velocities was traversed for a specific angle of attack. A typical result obtained in this way is depicted in Fig. 6 for the square wing in the form of a graph of the rolling moment coefficient $C_L = L/(\rho V^2 As/2)$ vs. the dimensionless roll angular velocity Ω_x with the angle of attack α as a parameter. The values given are the ones actually measured, i.e. with Ω_x expressed relative to the longitudinal axis of the wind tunnel, while C_L was measured about the fixed longitudinal axis of the model. The axes were not converted, since the correction is small in the range investigated for angle of attack. As a comparison, the calculated result from Truckenbrodt's linear airfoil theory is also entered.

It was found that the rolling moment C_L was tangent to the result of the linear theory at $\Omega_x = 0$ for $\alpha = 0°$. As Ω_x increases, C_L grows faster than the linear-theory result, producing considerable differences for large Ω_x. The rolling damping $\partial C_L/\partial \Omega_x$ as the derivative of the rolling moment coefficient with respect to Ω_x is thus no longer constant, as it is assumed to be in the linear theory, but is a function of Ω_x.

For the angle of attack $\alpha = 1°$, the rolling moment is initially linear with a larger slope than in the case of the linear theory. This corresponds to a larger rolling damping than that given by the linear theory. Above the value $\Omega_x = 0.065$, the straight line transposes to a curve of progressively larger curvature. A similar picture is obtained for $\alpha = 2°$, with an initially linear behavior with a greater slope, transposing at

$\Omega_x = 0.08$ to the previously observed curve.

As the angle of attack continues to grow, only straight lines are obtained in the measured range of Ω_x, corresponding to a constant rolling damping independent of roll angular velocity. At $\alpha = 10°$, a further increase in rolling damping can be observed, while at that point, it begins to decrease -- this is not shown in the diagram. /7

Curves similar to those obtained here for the square wing were also measured for the other wings. This can be seen from Fig. 7, in which the measured rolling dampings, normalized by the corresponding result of the linear theory, are plotted against angle of attack. The curve provided with the square symbols shows the behavior described above for the rolling damping of the square wing: in the region $0° < \alpha < 2°$, the rolling damping depends on the roll angular velocity, then rises to two or three times the linear result at $\alpha = 10°$, followed by a drop until at $\alpha = 20.5°$, the roll motion is no longer damped and transposes to the unstable region of autorotation.

The result for the wing with the taper ratio $\lambda = 0.5$ looks similar, but shows an even greater increase in rolling damping relative to the linear theory, while the drop of rolling damping into the unstable region is not as steep as in the case of the square wing. As the taper ratio is decreased further, the maximum of the rolling damping relative to the linear theory decreases and is shifted toward smaller angles of attack. Thus, in the case of the triangular wing, the maximum is only 1.4 times the linear rolling damping at an angle of attack of $\alpha = 6°$. Furthermore, the decrease of rolling damping in the region of large angles of attack is much less steep.

The observed phenomena, the dependence of rolling damping on the roll angular velocity for small angles of attack and the in part rapid rise in rolling damping with increasing angle of attack, cannot be explained with the aid of the linear theory. /8 It therefore seems likely that they are connected with the previously described separation phenomena and the formation of vortices above the suction side of the wing. In particular, the nonlinear curve of rolling moment in relation to roll angular velocity, which is reminiscent of the nonlinear lift characteristic of slender wings in symmetrical incident flow, strongly suggests this conclusion.

The causes for the partially curved and partially straight graph of rolling moment vs. roll angular velocity can be determined by observing the associated flow configurations.

By employing the paint procedure, we obtain a picture of the type of flow around the wing and thus an explanation for the different behavior of the rolling moment in the various regions.

Paint pictures were prepared with the wing (taper ratio $\lambda = 0.125$) for the following cases:

1. for a point on the curved section of a graph ($\alpha = 0°$, $\Omega_x = 0.10$)
2. for the point of transition from the straight to the curved section ($\alpha = 2.5°$, $\Omega_x = 0.10$)
3. for a point on the straight section of a curve ($\alpha = 2.5°$, $\Omega_x = 0.10$) [sic]

Figures 9 and 10 show these situations. First, the left part of Fig. 9 shows the paint picture of the suction side of a wing in a symmetrical airstream with $\alpha = 10°$ as well as the associated configuration of the rolled-up vortex layers. This is the known picture of two symmetrically positioned vortices.

In the paint picture, the presence of a vortex above the wing surface can be recognized by the dense clusters of s-shaped lines.

On the right is the paint picture of a wing rolling with /9
$\Omega_x = 0.10$ at $\alpha = 0°$. Looking closely at the right outer region, the presence of a vortex on the trailing part of the wing side away from the rolling motion can be detected by the s-shaped lines. When the wing turns by 180° about its longitudinal axis, precisely the same picture is obtained. Hence, the vortices are antisymmetrically positioned, as indicated in the sketch underneath. This vortex configuration is the consequence of the antisymmetric angle-of-attack distribution over the span of the wing induced by the rolling motion. It is no longer conical as in the case of a constant angle of attack, which can be recognized by the fact that a clear trace of the vortex is visible practically only in the trailing area of the wing. The depicted flow around the wing results in progressively increasing curvature in the graph of rolling moment vs. roll angular velocity.

If the angular velocity is held constant and the angle of attack increased, the vortex is intensified on the side of the wing which has a larger mean effective angle of attack resulting from the sum of the constant angle-of-attack distribution and the angle-of-attack distribution induced by the rolling motion, while it is weakened on the other half of the wing. With further increases in the angle of attack α, this leads to a state in which the airstream approaches one half of the wing on the average in the direction of the wing chord, so that no well-defined vortex separates along the entire edge, while the vortex separation along the other half of the wing has further intensified. This situation is depicted on the left in Fig. 10. The

presence of vortex separation along the entire edge can be quite clearly detected on the right half of the wing, while on the left, nothing of the sort can be observed both on the upper side and on the lower side, with the exception of minor local separation phenomena in the vicinity of the leading and trailing edges. This situation corresponds exactly to the previously discussed aspect of discontinuity.

If rotation is constant while the angle of attack is further /10
increased, a configuration is obtained corresponding to the right picture, where the dominance of the angle of attack α over the angle-of-attack distribution induced by the rolling motion results in the formation of two vortices of different intensities on one side of the wing. This situation corresponds to a linear dependence of rolling moment on roll angular velocity, i.e. constant rolling damping.

The observation of flow conditions in connection with the graph of rolling moment vs. roll angular velocity (Fig. 8) therefore leads to the conclusion that the antisymmetrical vortex configuration with two vortices on two sides of the wing corresponding to point A in Fig. 8 results in nonlinear behavior of rolling moment in relation to roll angular velocity, while the position of both vortices on one side of the wing produces a linear relationship (point C). The transition from one region to the other results from the transfer of a vortex from one side of the wing to the other (point B).

The increase in rolling damping with angle of attack can be explained by the different growths in the two separated vortices due to the difference in flow toward the two halves of the wing. Nevertheless, if the angle of attack α is greatly increased, the influence of the antisymmetric angle-of-attack distribution becomes smaller and smaller in relationship to the constant angle

of attack which is now substantially larger. The vortices over the two halves of the wing are equal in intensity, so that the differences in pressure distribution of the two wing halves are reduced, which results in the previously mentioned drop in rolling damping at large angles of attack. On the other hand, the steep drop in rolling damping for the square wing, which results in instability, can be attributed to the separation of flow from the leading edge.

The presence of leading-edge separation with the development of free vortices over the corresponding suction side of the wing can also be demonstrated by introducing smoke into the airstream. The result in Fig. 11 shows the situation in which vortex separation occurs only over one half of the wing, while the airstream approaches the other half (on the average) in the direction of the chord. For this reason, all of the smoke introduced concentrates in the center of the one vortex. /11

5. Comparison Between Theory and Measurement

In conclusion, we will report on the comparison of the measurements with theoretical calculations. Rolling moments were calculated from linear and nonlinear theories. The results are depicted in Fig. 12 for the square wing.

The straight line 1 is the result of Truckenbrodt's linear airfoil theory, which was employed earlier for comparisons. Curve 2 is a result obtained through application of Gersten's nonlinear airfoil theory [2] for the rolling wing. This theory utilizes a vortex model with free vortices leaving the wing surface at half the local angle of attack. It was found that the nonlinear theory provides relatively good agreement with the measurements for the square wing.

6. Summary

An experiment setup for measuring aerodynamic forces on airfoil models in rolling motion and the results obtained with it are reported. It was found that the wings investigated sometimes exhibited a highly nonlinear relationship between rolling moment and roll angular velocity, and rolling damping with a high dependence on angle of attack. This is due to the presence of leading-edge separation with the formation of /12
rolled-up vortices over the wing surface. The different configurations of vortices and the resulting effects on rolling damping were discussed and, whenever possible, compared with theoretical approaches.

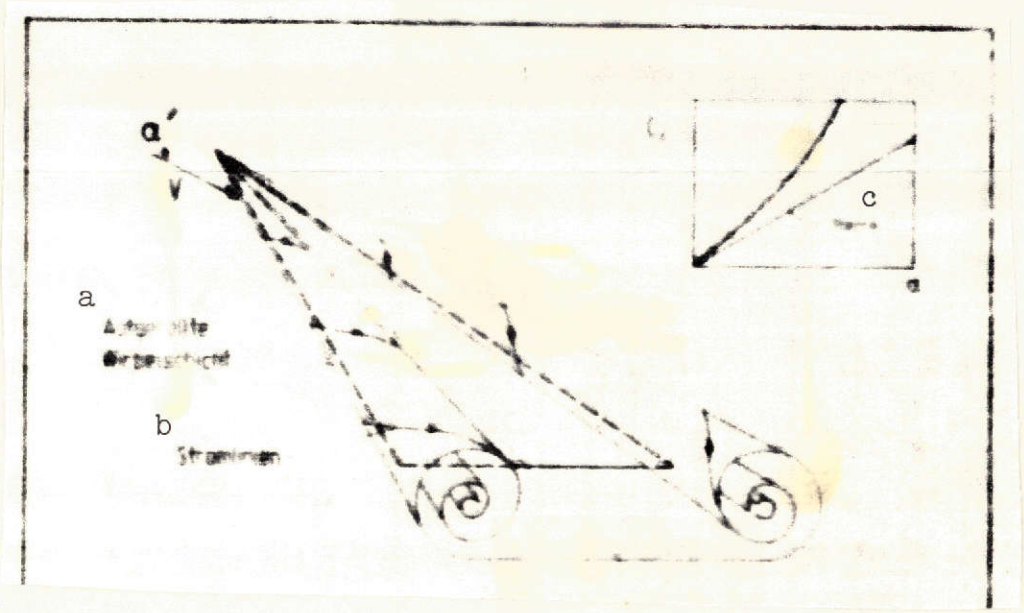

Fig. 1. Vortex formation for a sharp-edged delta wing.

Key: a. Rolled-up vortex layer
b. Streamlines
c. Theory

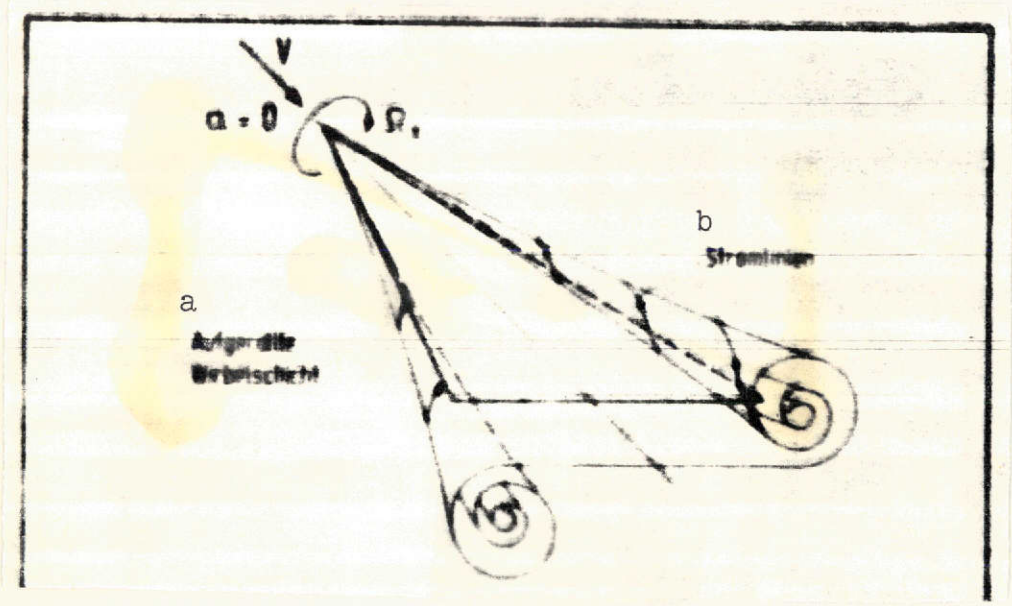

Fig. 2. Vortex formation for a rolling wing.

Key: a. Rolled-up vortex layer
b. Streamlines

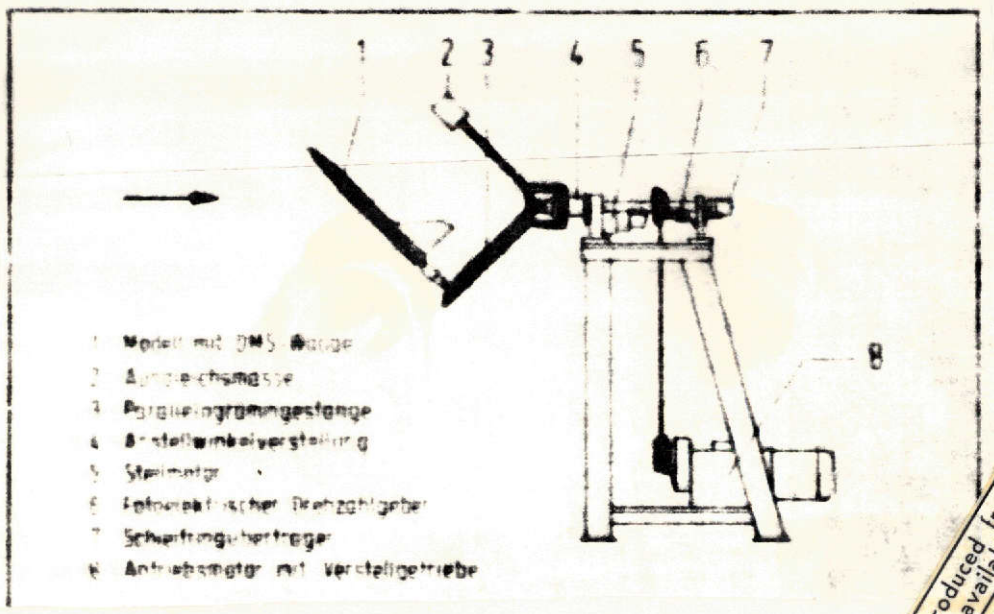

Fig. 3. Roll balance (schematic).

Key: 1. Model with strain gauge balance
2. Counterweight
3. Paralellogram linkage
4. Angle-of-attack adjustment
5. Servomotor
6. Photoelectric tachometer
7. Slip-ring contact
8. Drive motor with control gear

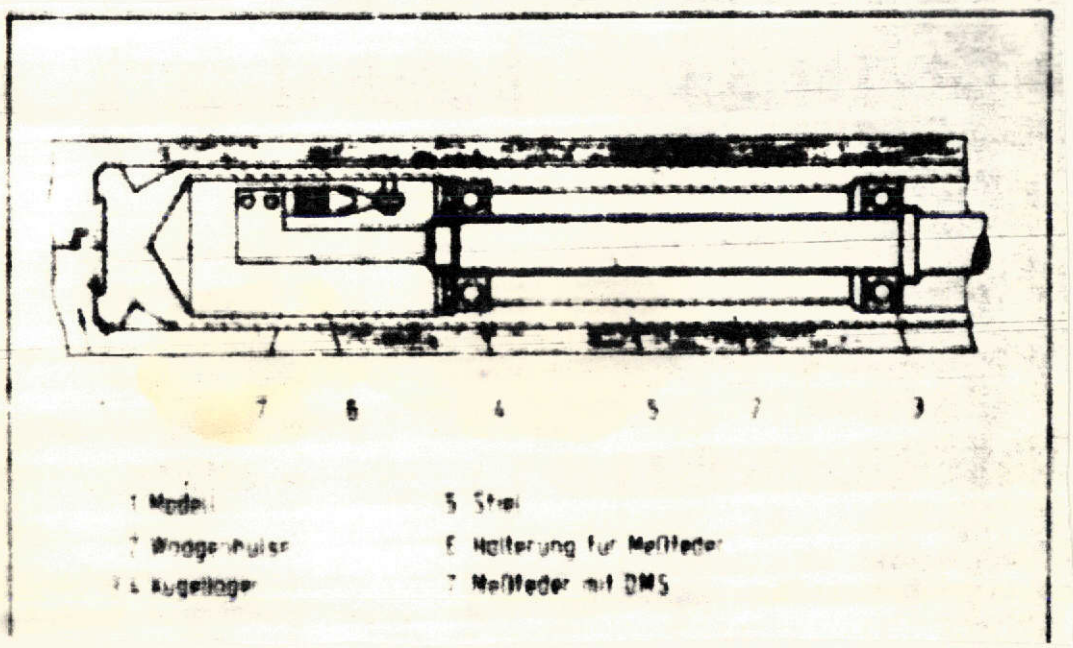

Fig. 4. Construction of rolling-moment balance (schematic).

Key: 1. Model
2. Balance sleeve
3,4. Ball bearings
5. Shaft
6. Attachment for measuring spring

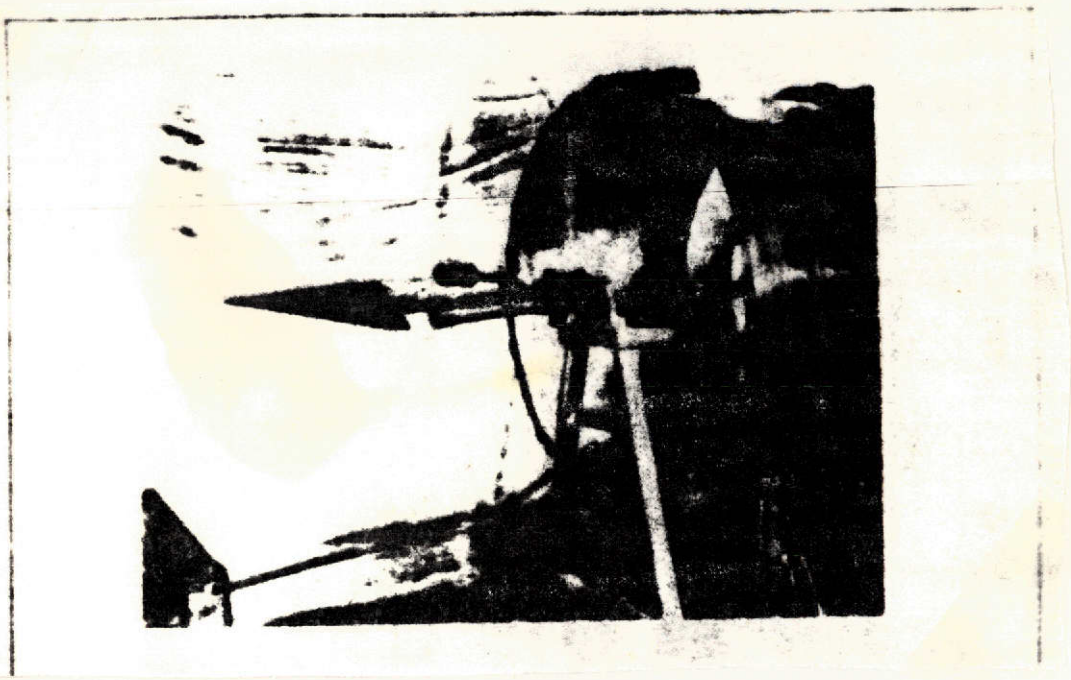

Fig. 5. Roll balance in 1.3-m-diameter wind tunnel.

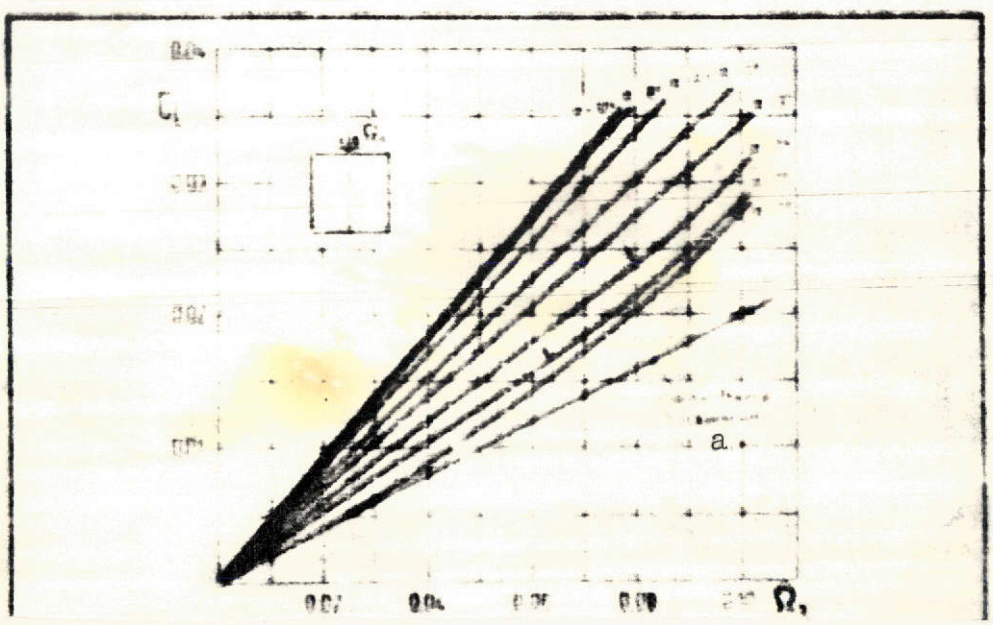

Fig. 6. Rolling moment C_L in relation to roll angular velocity Ω_x.

Key: a. Linear theory

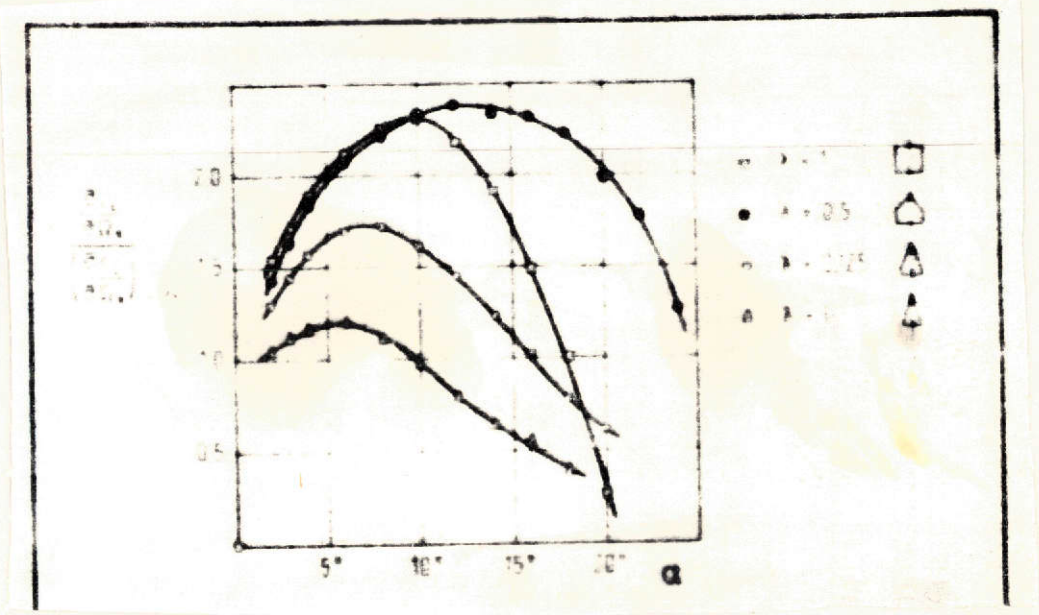

Fig. 7. Rolling damping in relation to angle of attack.

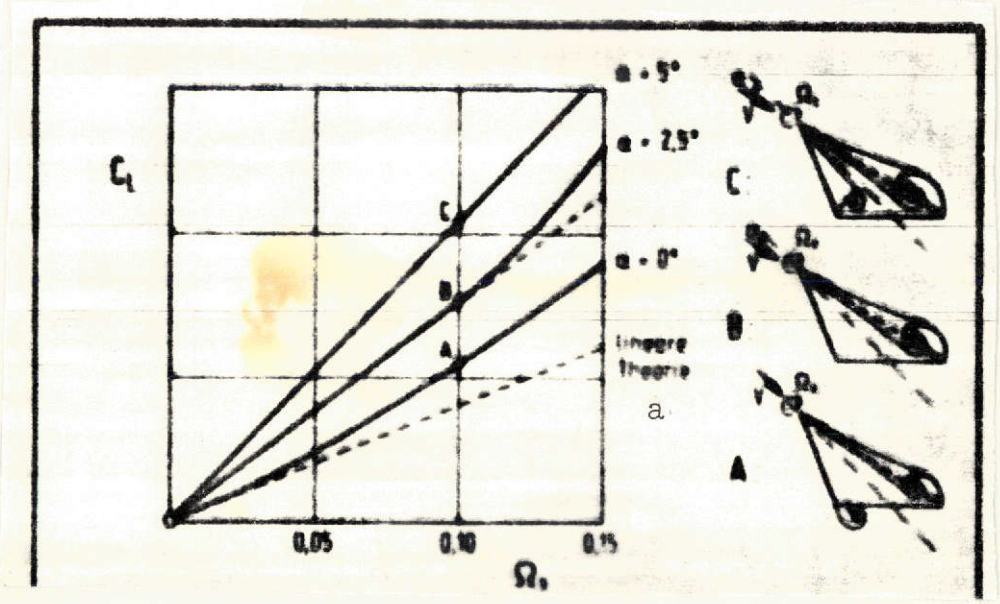

Fig. 8. Influence of vortex configuration on rolling moment.

Key: a. Linear theory

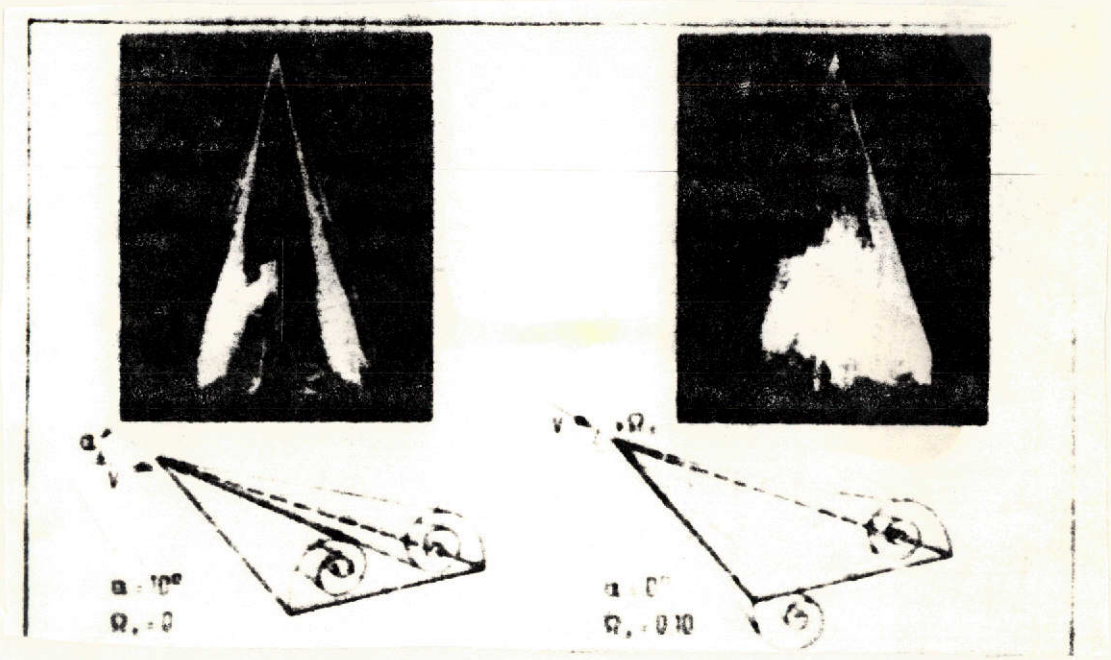

Fig. 9. Configuration of separated vortex surfaces on rotating wing.

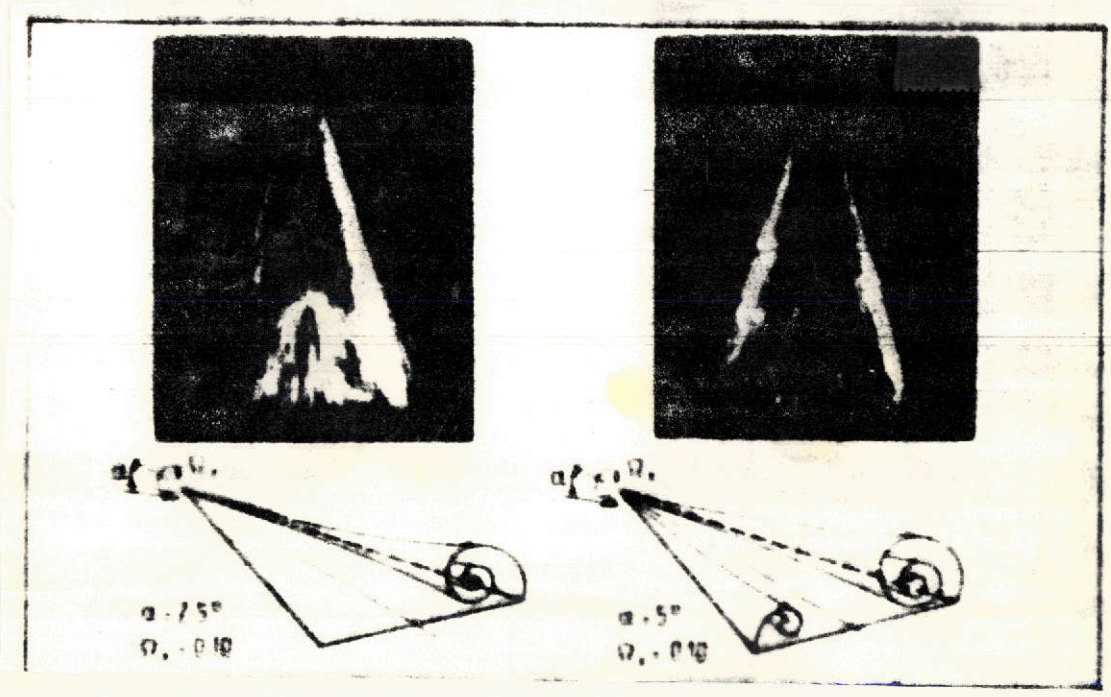

Fig. 10. Configuration of separated vortex surfaces on rotating wing.

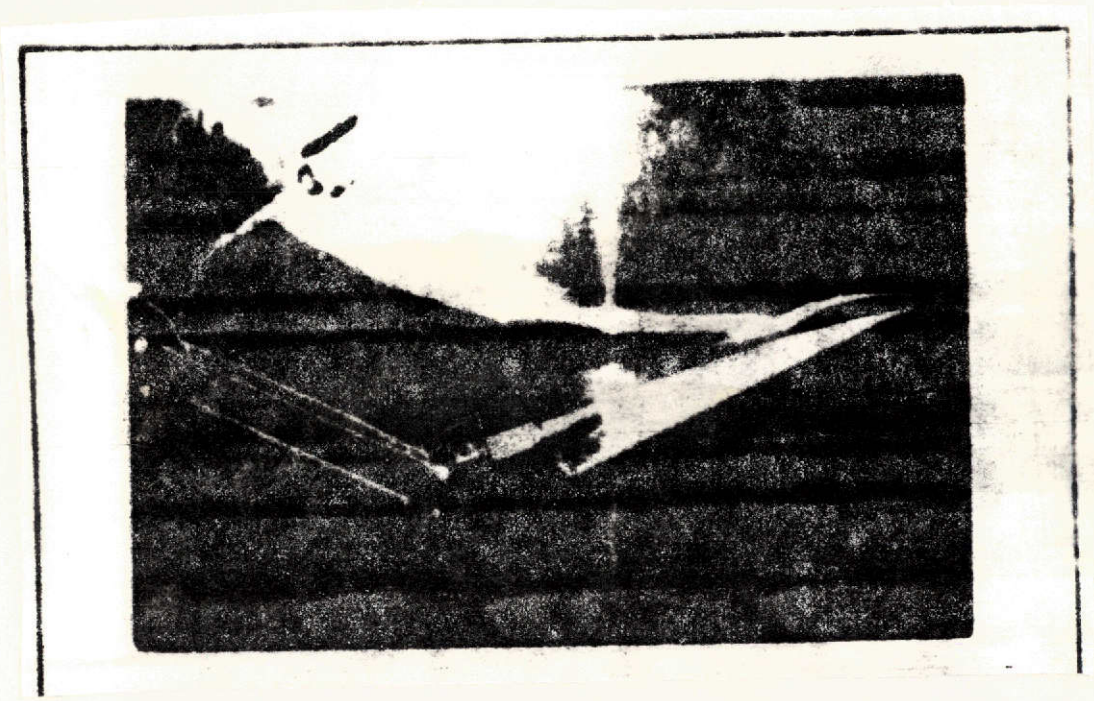

Fig. 11. Vortex formation on rotating wing.

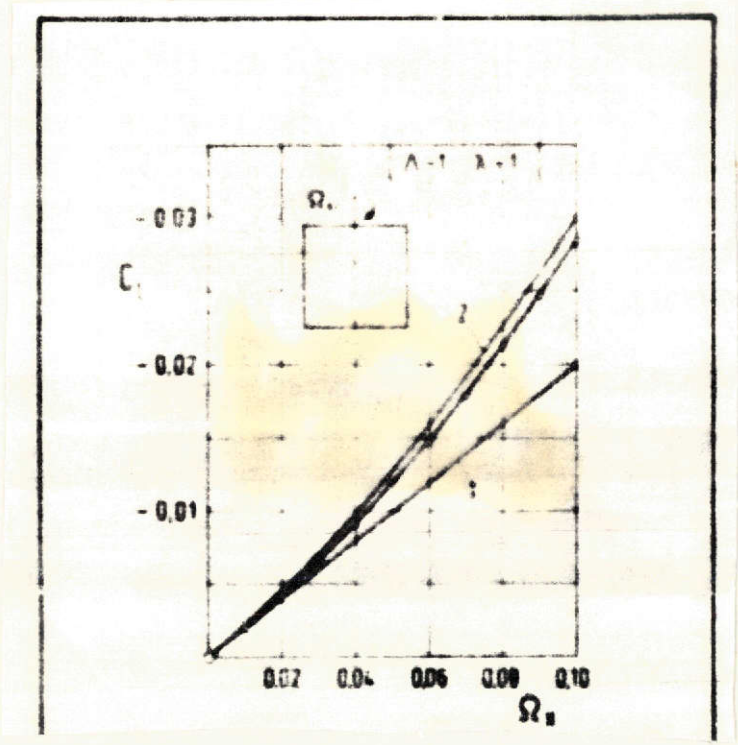

Fig. 12. Comparison between theory and measurement for $\alpha = 0°$.

° Measurements with roll balance
1 Truckenbrodt's linear theory
2 Gersten's nonlinear theory

REFERENCES

1. Hummel, D., "Experimental investigation of flow on suction side of slender delta wing," ZfW 13, 247-252 (1965).

2. Gersten, K., "Nonlinear airfoil theory, particularly for airfoils with small side ratio," Ing.-Archiv. 30, 431-452 (1961).

3. Harvey, J.K., "A study of the flow field associated with a steadily rolling slender delta wing," J. of the Royal Aeron. Soc. 68, 106-110 (1964).

4. Klinke, E., "Multi-component built-in balances for measurements on rotating models," WGLR Report No. 8/1963; Report on third meeting of Subcommittee on Aerodynamic Measuring Techniques, Jan. 24, 1962, in Braunschweig.

   see also: Klinke, E. and A. Muller, "Contribution to measuring rolling damping in a wind tunnel," Jahrbuch 1962 der WGLR [1962 Annual of the WGLR], pp. 167-170.